MESON PRODUCTION AND BARYON RESONANCES AT CLAS *

VOLKER D. BURKERT

Jefferson Lab, 12000 Jefferson Avenue, 12000 Jefferson
Newport News, Virginia, 26000, USA
burkert@jlab.org

I give a brief overview of the exploration of baryon properties in meson photo- and electroproduction. These processes provide ample information for the study of electromagnetic couplings of baryon resonances and to search for states, yet to be discovered. The CLAS detector, combined with the use of energy-tagged polarized photons and polarized electrons, as well as polarized targets and the measurement of recoil polarization, provide the tools for a comprehensive nucleon resonance program. I briefly present the status of this program, prospects for the next few years, and plans for the Jefferson Lab 12 GeV upgrade.

Keywords: baryon resonances; photoproduction; transition form factors, polarization

PACS numbers 1.55Fv, 13.60Le, 13.40Gp, 14.20Gk

1. Introduction

The systematics of the baryon excitation spectrum is key to understanding the effective degrees of freedom underlying the nucleon matter[1]. The most comprehensive predictions of the resonance excitation spectrum come from the various implementation of the constituent quark model based on broken $SU(6)$ symmetry[2]. Gluonic degrees of freedom may also play a role[3], and resonances may be generated dynamically through baryon-meson interactions[4]. Recent developments in Lattice QCD led to predictions of the nucleon spectrum in QCD with dynamical quarks[5], albeit with still large pion masses of 420 MeV. In parallel, the development of dynamical coupled channel models is being advanced with new vigor. The EBAC group at JLab has demonstrated[6] that coupled channel effects result in a large mass shift for the Roper resonance downward from the bare core mass of 1736 MeV to 1365 MeV, explaining the low physical mass of the state.

The various resonance models not only predict different excitation spectra but also different Q^2 dependence of transition form factors. Mapping out transition form factors in meson electroproduction experiments can tell us a great deal about the effective degrees of freedom underlying baryon structure.

2

2. Search for new excited nucleon states

It is well recognized that the analysis of differential cross sections in the photoproduction of single pseudoscalar mesons alone results in ambiguous solutions for the contributing resonant partial waves. The N^* program at JLab is aimed at complete, or nearly complete measurements for processes such as $\vec{\gamma}\vec{p} \to \pi N$, ηp, $K^+\vec{Y}$ and $\vec{\gamma}\vec{n} \to \pi N$, $K^\circ\vec{\Lambda}$. These reactions are fully described by four complex parity-conserving amplitudes, which may be determined from eight well-chosen combinations of unpolarized cross sections, and single and double polarization observables using beam, target, and recoil polarization measurements. If all combinations are measured, 16 observables can be extracted providing highly redundant information for the determination of production amplitudes.

A large part of the experimental program makes use of the CLAS detector[7], which provides particle identification and momentum analysis in a polar angle range from $8°$ to $140°$. The photon energy tagger provides energy-marked photons with an energy resolution of $\frac{\sigma(E)}{E} = 10^{-3}$. Circularly polarized photons are generated by scattering the highly polarized electron beam from an amorphous radiator. Other equipment includes a coherent bremsstrahlung facility with a precision goniometer for diamond crystal positioning and angle control. The facility has been used for coherent photon bremsstrahlung production, generating photons with linear polarization up to 90%. There are two frozen spin polarized targets, one based on butanol as target material (FROST), and one using frozen HD as target material (HDIce). FROST has been operated successfully. An production run of 5 months has been completed in August 2010. The HDIce target is currently being assembled. It has better dilution factor and will serve as polarized neutron target. It is scheduled to take data in 2011 and 2012.

In hyperon channels, very precise cross section and polarization data have been measured[8,9,10,11,12,13,14]. In channels involving nucleons in the final state where the recoil polarization is usually not measured, seven independent observables are obtained directly. The recoil polarization can be inferred from a beam-target double polarization measurement. Precise measurements of differential cross section for π°, π^+, π^- η, η', and ω have been published[15,16,17], while analyses of polarization observables for these reactions are in progress. For $p\omega$ production, the $\omega \to \pi^+\pi^-\pi^\circ$ decay distribution contains polarization information, providing additional information that constrain the partial wave analysis. In CLAS, the final state is fully determined by measuring the charged pions, and inferring the π° through kinematical constraints. Fig. 1 shows the spin density matrix elements for $\gamma p \to p\omega$. Results of the partial wave fit are shown in Fig. 2. The fit to the phase motion of dominant partial waves requires inclusion of 3 well known resonances, $F_{15}(1680)$, $D_{13}(1700)$, $G_{17}(2190)$), as well as the quark model state $F_{15}(2000)$, an unconfirmed 2-star state in RPP[18].
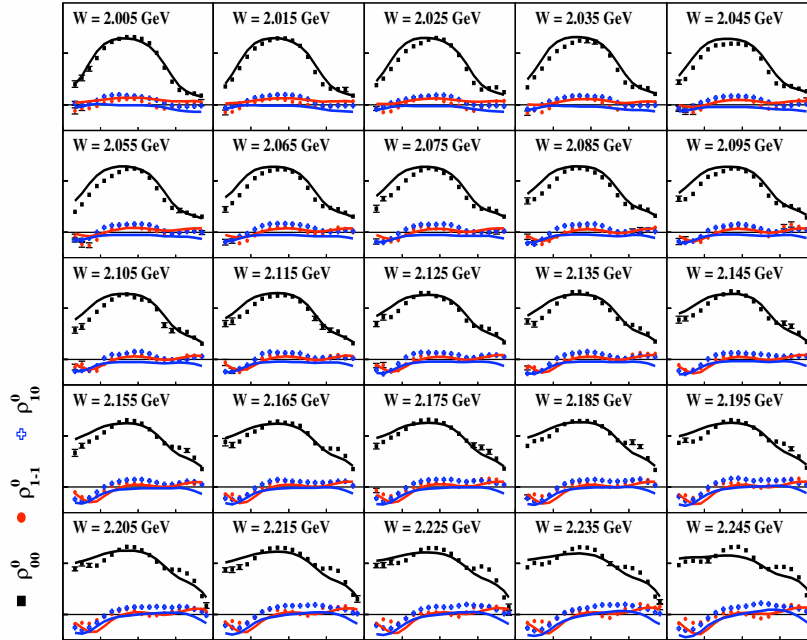
Fig. 1.   Angular dependence in the range $-1 < cos\theta^* < 1$ for spin density matrix elements ρ^0_{00}, ρ^0_{10}, and ρ^0_{1-1} of the process $\gamma p \rightarrow p\omega$, in the mass range from 2 to 2.25 GeV.

3. Electromagnetic excitation of nucleon resonances

Electromagnetic transition form factors encode information about the transition charge and magnetization densities[19], which in turn reflect the electromagnetic structure of the excited states. The non-relativistic constituent quark model (nr-CQM) provides a reasonable representation of the mass spectrum of many excited states below 2 GeV. Relativized versions, e.g. in ref. [20], give qualitative agreement with some of the measured transition amplitudes. The $N(1440)P_{11}$, or "Roper" resonance, however, has escaped description within this approach. The constituent quark model represents this state as a radial excitation of the nucleon, but has difficulties to describe its basic features such as the mass, photocouplings, and Q^2 evolution. In fact, the photocoupling amplitude has the wrong sign, and its magnitude is predicted to rise strongly at small Q^2 contrary to the data that show a rapid drop.
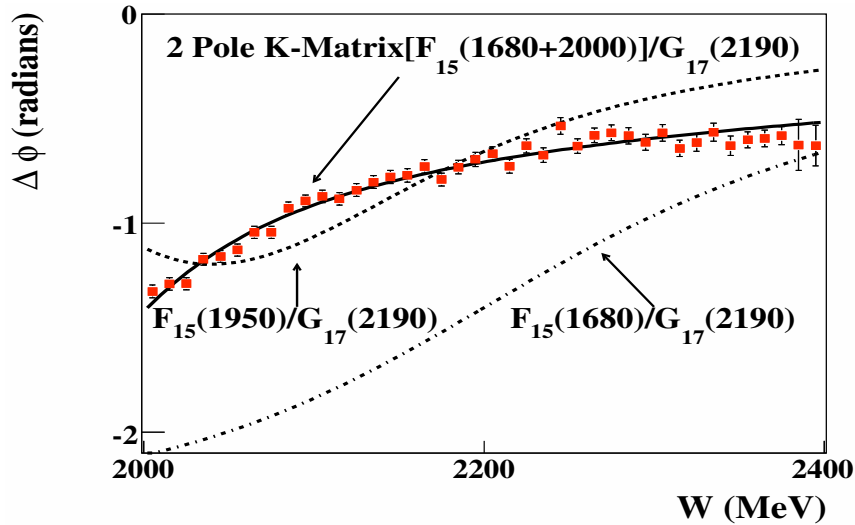
4

Fig. 2.   Fit results for $\Delta\phi = \phi_{7/2^-} - \phi_{5/2^+}$ vs the invariant $p\omega$ mass. The dot-dashed line is the phase motion expected using constant width Breit-Wigner distributions and the parameters quoted by the PDG for the $F_{15}(1680)$ and $G_{17}(2190)$. The dashed line required the $J^P = 7/2^-$ parameters to be within the PDG limits for the $G_{17}(2190)$, while allowing the $J^P = 5/2^+$ parameters to vary freely. The solid line used a constant width Breit-Wigner distribution for the $G_{17}(2190)$, but a 2-pole single channel K-matrix for the $J^P = 5/2^+$ wave.

3.1. *The Roper resonance*

The problems with describing the $N(1440)P_{11}$ "Roper" in constituent quark models has prompted the development of alternative models involving gluon fields[3], or meson-baryon degrees of freedom[21,22], and light-cone quark model[23,24]. In particular, measurements of its transition amplitudes in pion electroproduction has revealed information about the nature of the state.

Given these different theoretical concepts for the structure of the state, the question "what is the nature of the Roper state?" has been a focus of the N^* program with CLAS. The state is very wide, and pion electroproduction data covering a large range in the invariant mass W with full center-of-mass angular coverage are key in extracting the transition form factors. As an isospin $I = \frac{1}{2}$ state, the $P_{11}(1440)$ couples more strongly to $n\pi^+$ than to $p\pi^\circ$. Also, contributions of the high energy tail of the $\Delta(1232)$ are much reduced in that channel due to the $I = \frac{3}{2}$ nature of the $\Delta(1232)$. Previous studies[25] have mostly used the $p\pi^0$ final state from measurements focussing on the $\Delta(1232)$ mass region. Recently published analysis by the CLAS collaboration included new high statistics $n\pi^+$ data[26] that covered the mass region from pion threshold to 1.7 GeV/c^2. In addition, large samples of differential cross section data[27,28,29] and polarization observables[30] taken earlier with CLAS
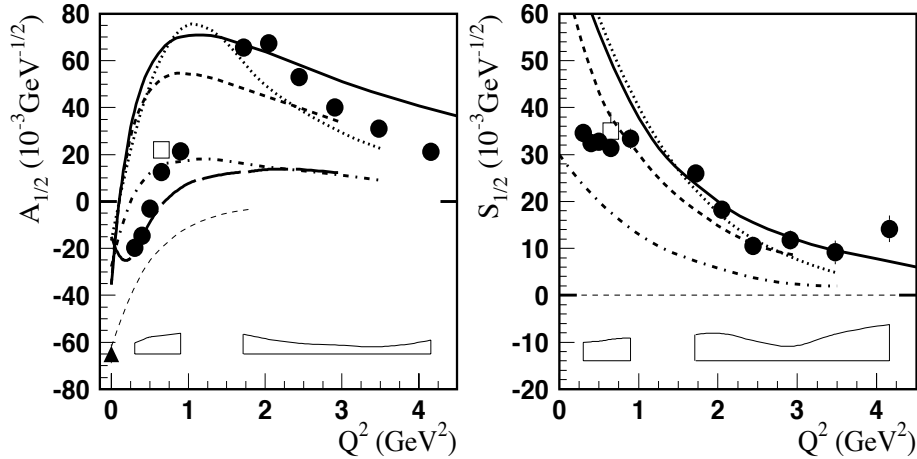
Fig. 3.   Transverse electrocoupling amplitude for the Roper $N(1440)P_{11}$ (left panel). The full circles are the new CLAS results. The squares are previously published results of fits to CLAS data at low Q^2. The right panel shows the longitudinal amplitude. The bold curves are all relativistic light front quark model calculations [24]. The thin dashed line is for a gluonic excitation[3].

in the channels $p\pi°$ and $n\pi^+$ are included in a comprehensive analysis of nearly 120,000 data points covering a large range in θ_π, ϕ_π, W, Q^2. Also, cross section data from $p\eta$ final state[31,32] were used to independently determine amplitudes of the transition to the $N(1535)S_{11}$ state. This allows one to constrain the branching ratio $\beta_{N\pi}$ and $\beta_{N\eta}$ for this state more accurately. Two independent approaches, fixed-t dispersion relations and the unitary isobar model, have been employed to estimate the model-sensitivity of the resulting transition amplitudes[33,34] for the three low mass states, $N(1440)P_{11}$, $N(1520)D_{13}$, and $N(1535)S_{11}$.

The transverse and longitudinal amplitudes $A_{1/2}$ and $S_{1/2}$ of the transition to the $N(1440)P_{11}$ resonance are shown in Fig. 3.1. At the real photon point $A_{1/2}$ is negative, rises quickly with Q^2, and changes sign near $Q^2 = 0.5$ GeV^2. At $Q^2 = 2$GeV^2 the amplitude reaches about the same magnitude but opposite sign as at $Q^2 = 0$, before it slowly falls off with Q^2. This remarkable sign change with Q^2 has not been observed before for any nucleon form factor or transition amplitude. At high Q^2, both amplitudes are qualitatively described by the light front quark models, which is consistent with the interpretation of the state as a radial excitation of the nucleon at short distances. The low Q^2 behavior is not well described by the LF quark models which fall short of describing the amplitude at the photon point. This suggests that important contributions, e.g. meson-baryon interactions describing the large distances behavior, are missing, as has also been recently demonstrated in a covariant valence quark model[36,37]. A first exploration of the Roper transition form factors has recently been undertaken within Lattice QCD[35].

6

3.2. *Strangeness electroproduction*

Electroproduction cross section measurements of strangeness channel, e.g. $ep \rightarrow eK^+Y^\circ$, and polarization transfer measurements $\vec{e}p \rightarrow eK^+\vec{Y^\circ}$, ($Y^\circ = \Lambda$, Σ) have been carried out[38,39] that allow stringent tests of hadronic models. The separated structure functions reveal clear differences between the production dynamics for the Λ and Σ. No hadronic model has been able to reproduce the energy and angle dependences, which show indications of strong s-channel resonance behavior, especially in the case of the $K^+\Sigma^\circ$ channel. These data will provide important constraints for dynamically coupled-channel analyses.

4. Conclusion & Outlook

A large effort is currently underway with CLAS at Jefferson Lab to probe the S=0 baryon excitation spectrum in photo- and electroproduction measurements of varies baryon-meson final states. These include cross sections and many polarization observables, both with polarized beam and polarized targets, as well as recoil polarization measurements. Measurement on polarized proton targets have been completed with an extended run in 2010. The program on the neutron is planned to be completed with a photon run using polarized HD material in 2011/2012. The determination of transition amplitudes for many high-mass states is ongoing. Precise transition amplitudes have been published for the low-mass resonances. The 2-pion final state is being analyzed to study both low mass states[40] and higher mass states that dominantly couple to 2-pion channels such as $S_{31}(1620)$, $D_{33}(1700)$ and others[41,42]. Lastly, a program to measure resonance transition form factors at $5 < Q^2 < 12$ GeV^2 has been approved for the CLAS12 detector[43] currently under construction at JLab as part of the 12 GeV energy upgrade of its electron accelerator.

References

1. For an overview see: V. Burkert and T.-S. H. Lee, Int. J. Phys. E13, 1035, 2004.
2. N. Isgur and G. Karl, Phys. Rev. D18, 4187, 1978; Phys. Rev. D19, 2653, 1979.
3. Z.P. Li, V. Burkert, Zh. Li; Phys .Rev. D46, 70, 1992.
4. E. Oset et al., Int. J. Mod. Phys. A20:1619-1626, 2005.
5. J. M. Bulava et al., Phys. Rev. D 79, 034505 (2009)
6. H. Kamano, S.X. Nakamura, T.-S.H. Lee, T. Sato, Phys. Rev. C 81, 065207 (2010).
7. B. Mecking et al., Nucl. Instrum. Meth. A503, 513-553, 2003.
8. J. W. McNabb et al., Phys. Rev. C69, 042201, 2004.
9. R. Bradford et al., Phys. Rev. C 73, 035202, 2006; Phys. Rev. C75, 035205, 2007.
10. I. Hleiqawi et al., Phys. Rev. C75, 042201, 2007,Erratum-ibid.C76:039905,2007.
11. M. McCracken et al., Phys. Rev. C81, 025201, 2010.
12. S. Anafalos Pereira et al., Phys. Lett. B688, 289, 2010.
13. B. Dey et al., Phys. Rev. C82, 025202, 2010.
14. L. Guo et al., Phys. Rev. C76, 025208, 2007.
15. M. Dugger et al., Phys. Rev. Lett. 89, 222002, 2002; Phys. Rev. Lett. 96, 062001, 2006; Phys. Rev. C76, 025211, 2007; Phys. Rev. C79, 065205, 2009.

16. W. Chen et al., Phys. Rev. Lett. 103, 01230.
17. M. Williams et al., Phys. Rev. C 80, 065208, 2009; Phys. Rev. C 80, 065209, 2009; Phys. Rev. C 80, 045213, 2009.
18. C. Amsler et al. (Particle Data Group), Phys. Letts. B 667, 2008.
19. L. Tiator and M. Vanderhaeghen, Phys. Lett. B672, 344-348, 2009.
20. M. Aiello, M.M. Giannini, and E. Santopinto, J. Phys. G24, 753, 1998.
21. F. Cano and P. Gonzales, Phys. Lett. B431, 270, 1998.
22. O. Krehl, et al., Phys.Rev.C62,025207, 2000.
23. S. Capstick and B.D. Keister, Phys. Rev. D51, 3598, 1995.
24. For an overview, see: I. Aznauryan, Phys. Rev. C76, 025212, 2007.
25. D. Drechsel, et al., Eur. Phys. J.A34, 69, 2007.
26. K. Park et al., Phys.Rev.C77,015208, 2008.
27. K. Joo, et al, Phys. Rev. Lett. 88, 122001, 2002; Phys. Rev. C68 032201, 2003; Phys. Rev. C70, 042201, 2004; Phys. Rev. C72, 058202, 2005.
28. H. Egiyan et al., Phys. Rev. C73, 025204, 2006.
29. M. Ungaro et al., Phys. Rev. Lett.97, 112003, 2006.
30. A. Biselli et al., Phys. Rev. C68, 035202, 2003; Phys. Rev. C78, 045204, 2008.
31. R. Thompson et al., Phys. Rev. Lett. 86, 1702, 2001.
32. H. Denizli et al. , Phys. Rev. C76, 015204, 2007.
33. I. Aznauryan et al., Phys. Rev. C78, 045209.
34. I. Aznauryan et al., Phys. Rev. C80, 055203, 2009.
35. H.-W. Lin et al, Phys.Rev.D78,114508,2008.
36. G. Ramalho and K. Tsushima, Phys.Rev.D81:074020,2010.
37. G. Ramalho, F. Gross, M.T. Pena, and K. Tsushima, arXiv:1008.0371 [hep-ph]
38. P. Ambrozewicz et al., Phys. Rev. C75, 045203, 2007.
39. D. Carman et al., Phys. Rev. Lett. 90, 131804, 2003; Phys. Rev. C79, 065205, 2009.
40. G.V. Fedotov et al., Phys. Rev. C79, 015204, 2009.
41. M. Ripani et al., Phys. Rev. Lett. 91, 022002, 2003.
42. V. Mokeev et al., Phys. Rev. C80, 045212, 2009.
43. V. D. Burkert, arXiv:0810.4718 [hep-ph]